2016 23rd International Conference on Pattern Recognition (ICPR)
Cancún Center, Cancún, México, December 4-8, 2016

Exposing Seam Carving Forgery under Recompression Attacks by Hybrid Large Feature Mining

Qingzhong Liu
Department of Computer Science
Sam Houston State University
Huntsville, TX 77341, USA
liu@shsu.edu

Abstract— **While seam carving has been widely used in computer vision and multimedia processing, it is also used for tampering illusions. Although several methods have been proposed to detect seam carving-based forgery, to this date, the detection of the seam carving forgery under recompression attacks in JPEG images has not been explored. To fill this gap, we proposed a hybrid large scale feature mining-based detection method to distinguish the doctored JPEG images from the untouched JPEG images under recompression attacks. Over one hundred thousand features from the spatial domain and from the DCT transform domain are extracted. Ensemble learning is used to deal with the high dimensionality and to avoid overfitting that may occur with some traditional learning classifier for the detection. Our study demonstrates the efficacy of proposed approach to exposing the seam-carving forgery under recompression attacks, especially from a lower quality level or on the same quality recompression.**

Keywords—seam carving; recompression, image forgery; big feature mining

I. INTRODUCTION

Seam carving, also known as image retargeting, content-aware scaling, liquid resizing or liquid rescaling, is a method developed by Shai Avidan and Ariel Shamir for image resizing [1]. The idea behind the image resizing is to establish a number of paths of least importance, called seams in an image or video file for both reduction and expansion. A seam is an optimal 8-connected path of pixels on a single image from top to bottom, or left to right. Seam carving allows manually defining areas in which pixels may not be changed and features the ability to erase entire objects from an image/photo. Seam carving has been implemented in Adobe Photoshop and other popular computer graphic applications including GIMP, digiKam, ImageMagic, and iResizer [14]. The proliferation of seam carving rises a serious challenge in image forensics.

JPEG is a commonly used method of lossy compression for digital images and many images/photos are saved or encoded in JPEG. Many image tampering operations involve JPEG images, JPEG image forensics has been widely explored in image forensics community. For example, Farid proposed a method to expose image forgery from JPEG ghost [5] and he also provided a comprehensive survey for image forgery detection [4].

Regarding seam carving–based image forgery detection, Sarkar et al. [12] utilized a steganalysis detector, originally developed to detect JPEG-based steganograms by Shi et al. [13], to expose seam-carved (or seam-inserted) from untouched images. Fillion and Sharma [6] designed a method to detect seam-carved images including benign image reduction, benign image enlargement, and deliberate image reduction. They tested their method over a set of images consisting of 1484 uncompressed images. Unfortunately, the JPEG images after content-aware manipulation were not tested. Inspired by the idea in detecting cropping and recompression as well as relevant copy-paste forgery [16], Liu and Chen also applied neighboring joint density that was used in steganalysis [9] and the calibrated version to detect seam carving-based forgery in JPEG images and obtained promising detection performance [10]. Chang et al. proposed a method to detect seam carving in JPEG images based on the symmetrical property of blocking artifact characteristics matrix (BCAM) and the extension [18]. Wei et al. proposed a patch analysis method to detect seam carving [20], Ryu and Lee designed a method to discriminate seam carving from intact by energy bias and noise features [19]. Recently, Yin et al. proposed a method to expose seam carving forgery by combining half-seam features, energy bias and noise-based feature from the local binary pattern [21].

Although several detectors have been used to detect seam carving-based image forgery, the effort to expose the tampering of low quality images is still missing. A crafty forgery maker may save doctored images/photos into a low quality. It becomes very hard to expose the forgery in low quality image. To resolve the problem, we design large scale features and utilize ensemble learning for the detection. Our experimental results prove the effectiveness of our approach.

In the followings, section 2 describes the background and the problem, section 3 states our detection methods, section 4 presents our experiments and analysis, followed by conclusions in section 5.

978-1-5090-4846-5/16/$31.00 ©2016 IEEE

II. Seam Carving Forgery under Recompression Attack

In seam carving, to achieve content-aware scaling, unnoticeable pixels on the least important seams that blend with their surroundings are removed or inserted. Formally, let I be an $n \times m$ image and a vertical seam is defined by:

$$S^X = \{s_i^x\}_{i=1}^n = \{(x(i), i)\}_{i=1}^n, \quad \text{s.t. } \forall i, |x(i) - x(i-1)| \le 1 \tag{1}$$

where x is a mapping $x : [1,..., n] \to [1,..., m]$. Similarly, a horizontal seam is defined by:

$$S^Y = \{s_j^y\}_{j=1}^m = \{(j, y(j))\}_{j=1}^m, \quad \text{s.t. } \forall j, |y(j) - y(j-1)| \le 1 \tag{2}$$

where y is a mapping $y : [1,..., m] \to [1,..., n]$.

The pixels of the path of seam S is denoted as $\mathbf{I}_s$. Given an energy function e, the cost of a seam is calculated by $E(s) = E(I_S) = \sum_{i=1}^n e(I(S_i))$. The optimal seam s^* generally minimizes the seam cost:

$$s^* = \min_S E(s) = \min_S \sum_{i=1}^n e(I(s_i)) \tag{3}$$

In the reference [1], several image importance measures are examined as the energy function. Although no single energy function performs well across all images but in general the following two measures e_1 and e_{HoG} work quite well.

$$e_1(I) = \left|\frac{\partial}{\partial x} I\right| + \left|\frac{\partial}{\partial y} I\right| \tag{4}$$

$$e_{HoG}(I) = \frac{\left|\frac{\partial}{\partial x} I\right| + \left|\frac{\partial}{\partial y} I\right|}{\max\left(HoG\left(I(x, y)\right)\right)} \tag{5}$$

Where $HoG\left(I(x, y)\right)$ is a histogram of oriented gradients at every pixel [15].

While seam carving has been widely used for content aware image resizing, it is also used for tampering illusion such as removing or inserting some objects. Figure 1 shows one untouched image on the left and doctored image by seam carving on the right.

Fig. 1. An example of image tampering by seam carving.

As we know, JPEG is a commonly used compression method for digital images. While a JPEG digital image is manipulated in spatial domain and then saved in JPEG format, it undergoes double compression. The detection of JPEG double compression has been well investigated in multimedia forensics. Given original JPEG image quality QF_1 (before tampering) and the manipulated image quality QF_2 (after tampering and saving in JPEG format), while the quality QF_2 is higher than QF_1, the detection of such a JPEG double compression is generally effective, however, while the quality QF_2 is lower than QF_1, most detection methods do not perform well. For example, in the experimental results in detecting JPEG double compression by using the methods in [2, 3, 11], while the first compression quality factor QF1 is higher than 77 and the second compression factor QF2 is lower than 57, all values of detection accuracy are only about 50%.

According to the inefficacy of most existing JPEG double compression detection algorithms in the detection while the quality QF_2 is lower than QF_1, and the underperforming or no exhibition in exposing the seam carving forgery in JPEG images while the quality QF_2 is lower than QF_1, a crafty forgery maker may process a JPEG image by the operation of seam carving in spatial domain and store the manipulated JPEG image at a lower quality. In such a manipulation, the following low-quality JPEG recompression may significantly destroy or compromise the traces left by seam carving. To our knowledge, while the manipulated images are saved at a lower-level JPEG quality, the examination has not been investigated. In other words, no effort has been literally marked in detecting the seam carving forgery with second lower quality JPEG compression.

In this paper, we aim to expose original seam carving forgery manipulation under recompression attacks especially from the low level quality JPEG recompression. Specifically, if we have two types of JPEG images with the same high level quality, one type is directly recompressed at a lower image quality, and another one is manipulated by seam carving and then recompressed at the same lower quality, we aim to determine which type of images was originally manipulated by seam carving. We propose the following hybrid large scale feature mining-based approach to discriminating seam carving forgery from untouched.

III. Large Feature Mining for the Detection

A. Large Derivative and Energy Features

Image intensity change over the image is important information in image analysis and computer vision that has been used for many applications. The intensity change is described with the x and y derivatives I_x and I_y, and the image gradient is the vector $\nabla I = [I_x, I_y]^T$. In this paper we expand the derivatives along different directions over different distances.

The derivative I_{ij} is defined the intensity change along the horizontal distance of i and along the vertical distance of j. Here the sum of i and j is the total offset distance of the derivative. We denote an image of size m×n by the pixel

matrix M,

$$M = \begin{bmatrix} a_{11} & a_{12} & \dots & a_{1n} \\ a_{21} & a_{22} & \dots & a_{2n} \\ \dots & \dots & \dots & \dots \\ a_{m1} & a_{m2} & \dots & a_{mn} \end{bmatrix},$$

The derivative matrix of I_{ij} is calculated by

$$M_{I_{ij}} = \begin{bmatrix} a_{11} - a_{(j+1)(i+1)} & a_{12} - a_{(j+1)(i+2)} & \dots & a_{1(n-i)} - a_{(j+1)n} \\ a_{21} - a_{(j+2)(i+1)} & a_{22} - a_{(j+2)(i+2)} & \dots & a_{2(n-i)} - a_{(j+2)n} \\ \dots & \dots & \dots & \dots \\ a_{(m-j)1} - a_{m(i+1)} & a_{(m-j)2} - a_{m(i+2)} & \dots & a_{(m-j)(n-j)} - a_{mn} \end{bmatrix}$$

$$= \begin{bmatrix} I_{ij}(1,1) & I_{ij}(1,2) & \dots & I_{ij}(1,n-i) \\ I_{ij}(2,1) & I_{ij}(2,2) & \dots & I_{ij}(2,n-i) \\ \dots & \dots & \dots & \dots \\ I_{ij}(m-j,1) & I_{ij}(m-j,2) & \dots & I_{ij}(m-j,n-i) \end{bmatrix} \quad (6)$$

Spatial derivative large feature mining contains the marginal density and neighboring joint density. For computational efficiency and feature reduction, our feature extraction is based on the derivative matrices, the algorithm is described below.

Derivative-based large feature mining algorithm

for d=1:max_d
for i=0:d
j=d-i;
% Marginal density features
% δ = 1 if its arguments are satisfied, otherwise 0
for h=0:max_h

$$MF_{ij}(h) = \frac{\sum_{r=1}^{m-j}\sum_{c=1}^{n-i}\delta\left(\left|I_{ij}(r,c)\right| = h\right)}{(m-j)(n-i)} \quad (7)$$

end
% Joint density features
for k=0:max_k
for l=0:max_l

$$NJH_{ij}(k,l) = \frac{\sum_{r=1}^{m-j}\sum_{c=1}^{n-i-1}\delta\left(\left|I_{ij}(r,c)\right| = k \;\&\; \left|I_{ij}(r,c+1)\right| = l\right)}{(m-j)(n-i-1)} \quad (8)$$

$$NJV_{ij}(k,l) = \frac{\sum_{r=1}^{m-j-1}\sum_{c=1}^{n-i}\delta\left(\left|I_{ij}(r,c)\right| = k \;\&\; \left|I_{ij}(r+1,c)\right| = l\right)}{(m-j-1)(n-i)} \quad (9)$$

end
end
end
end

In our study, we set the values of 8, 10, 10, and 10 to *max_d, max_h, max_k* and *max_l*, respectively. We obtain 484 marginal density features, and 10,648 joint density features, in a sub-total of 11,132 features.

Additionally, image filtering is applied to the image M, the filtered version is obtained. By applying the feature extraction algorithm to the filtered version, another 11,132 feature are obtained. We simply utilized image median filtering that could be further investigated and improved in the future study, as well as the optimal configuration of *max_d, max_h, max_k* and *max_l*.

In summary, we extract 22,264-D derivative features.

As we know, the optimal seams are examined by the least importance based on the energy function. We surmise that the seam carving operation changes the statistics of importance distribution. Therefore, we design the following features related the energy statistical features.

For the image M = $\{a_{ij}\}$ (i=1, 2… m; j=1, 2… n), and the parameters s_1 and s_2 are set by = 1, 2, 3, respectively. The sub set $X(s_1, s_2, d_1, d_2) = \{a_{ij}\}$ (i=s_1+d_1+1, s_1+d_1+2, …, s_1+d_1+m-max(s_1+d_1); j= s_2+d_2+1, s_2+d_2+2, …, s_2+n+d_2-max(d_2+s_2)). The differential matrices are constructed by:

$$e(d_1,d_2) = \sum_{(s_1,s_2)=(1,1)}^{(3,3)} \left|X(s_1,s_2,d_1,d_2) - X(2,2,d_1,d_2)\right| \quad (10)$$

$$e_1(d_1,d_2) = \min_{s_2=1,2,3}\left(\left|X(1,s_2,d_1,d_2) - X(2,2,d_1,d_2)\right|\right) \quad (11)$$

$$e_2(d_1,d_2) = \min_{s_2=1,2,3}\left(\left|X(3,s_2,d_1,d_2) - X(2,2,d_1,d_2)\right|\right) \quad (12)$$

$$e_3(d_1,d_2) = \min_{s1=1,2,3}\left(\left|X(s_1,1,d_1,d_2) - X(2,2,d_1,d_2)\right|\right) \quad (13)$$

$$e_4(d_1,d_2) = \min_{s1=1,2,3}\left(\left|X(s_1,3,d_1,d_2) - X(2,2,d_1,d_2)\right|\right) \quad (14)$$

Based on the differential matrix in equation (10), we extract the marginal density by

$$absM_e(p) = \frac{\delta(e(0,0) = p)}{(n-2)*(m-2)} \quad (15)$$

The neighboring joint density features are given by

$$absNJ^{1}_{e,d}(p,q) = \frac{\sum \delta\left(\left|e(0,0)\right| = p, \left|e(d_1,d_2)\right| = q\right)}{(n-d_1-2)(m-d_2-2)} \quad (16)$$

$$absNJ^{2}_{e}(p,q) = \frac{\sum \delta\left(\left|e_1(0,0)\right| = p, \left|e_2(0,0)\right| = q\right)}{(n-2)(m-2)} \quad (17)$$

$$absNJ^{3}_{e}(p,q) = \frac{\sum \delta\left(\left|e_3(0,0)\right| = p, \left|e_4(0,0)\right| = q\right)}{(n-2)(m-2)} \quad (18)$$

In equations (15), (16), (17) and (18), $\delta = 1$ if its arguments are satisfied, otherwise $\delta = 0$; the integer value of p and/or q is set from 0 to 10. In equation (16), the sum of d_1+d_2 is set from 1 to 7, there are 35 combinations of (d_1, d_2). We obtain a total of 4488 features.

Additionally, image filtering is applied to the image M, the filtered version is obtained. By applying the feature extraction from equations (15) to (18) to the filtered version, another 4488 feature are obtained.

In a subtotal, we obtain 8976 energy-based features.

B. Large Transform-Domain Features

The quantized DCT coefficient array of the image contains $B_1 \times B_2$ blocks. The F_{pq}-th block (p = 1, 2, …, B_1; q = 1, 2, …, B_2) consists of 8×8 quantized DCT coefficients. The coefficient at the frequency coordinate (u, v) of the block F_{pq} (u=0,1, …7, and v=0,1,…7) is denoted by $c_{pq}(u,v)$. The marginal density of the absolute coefficients is given by *absM*

$$absM\ (u,v;h) = \frac{\sum_{p=1}^{B_1}\sum_{q=1}^{B_2}\delta\left(\left|c_{pq}(u,v)\right| = h\right)}{B_1 B_2} \tag{19}$$

The individual frequency-based neighboring joint density on horizontal direction and vertical direction are given by:

$$absNJ_{1h}(u,v;x,y) = \frac{\sum_{p=1}^{B_1}\sum_{q=1}^{B_2}\delta\left(c_{pq}(u,v) = x \,\&\, c_{pq}(u,v+1) = y\right)}{B_1 B_2} \tag{20}$$

$$absNJ_{1v}(u,v;x,y) = \frac{\sum_{p=1}^{B_1}\sum_{q=1}^{B_2}\delta\left(c_{pq}(u,v) = x \,\&\, c_{pq}(u+1,v) = y\right)}{B_1 B_2} \tag{21}$$

The inter-block neighboring joint density on individual frequency band along the horizontal direction and vertical direction, the features are constructed as follows:

$$absNJ_{2h}(u,v;x,y) = \frac{\sum_{p=1}^{B_1}\sum_{q=1}^{B_2-1}\delta\left(c_{pq}(u,v) = x \,\&\, c_{p(q+1)}(u,v) = y\right)}{B_1(B_2-1)} \tag{22}$$

$$absNJ_{2v}(u,v;x,y) = \frac{\sum_{p=1}^{B_1-1}\sum_{q=1}^{B_2}\delta\left(c_{pq}(u,v) = x \,\&\, c_{(p+1)q}(u,v) = y\right)}{(B_1-1)B_2} \tag{23}$$

In equations (19) to (23), δ = 1 if its arguments are satisfied, otherwise δ = 0; h is the integer from 0 to 5, x and y are integers ranging from 0 to 4. The frequency coordinate pair (u, v) is set to (0,1), (1,0), (2,0), (1,1), (0,2), (0,3), (1,2), (2,1), (3,0), (4,0),(3,1),(2,2), (1,3), and (0,4), a subtotal of 84 marginal density features, 700 joint density features on the intra-block, and 700 joint density features on the inter-block.

The calibration features in the DCT domain is generated according to the following processing:

Decode the JPEG image under examination to spatial domain, which is denoted by matrix M. For d_1= 0 to 7, and d_2 = 0 to 7, while $(d_1,d_2) \neq (0,0)$:

1) Crop the matrix M by d_1 rows and d_2 columns in the spatial domain, and generate a shifted spatial image $M_{d_1 d_2}$ $(d_1, d_2) \in \{(0,1), \ldots, (0, 7), (1,0), \ldots, (7,7)\}$;
2) Compress the shifted spatial image $M_{d_1 d_2}$ to the JPEG format at the same quality factor;
3) Extract the marginal density and neighboring joint density features caculated by equations (19) to (23) respectively.

In the DCT domain, we extract 64*(84+700+700) = 94,976 features, denoted by **LF-DCT**(large features in DCT transform).

By integrating all features from both the spatial domain and the DCT domain together, a total of 126,216 features, denoted by **LF-DEDCT** (large features on Derivatives, Energy and DCT transform), are generated.

IV. Experiments

We have 3600 JPEG color images, encoded at the quality of '75'. The seam carving tool at http://code.google.com/p/seam-carving-gui/ is used to manipulate these JPEG images. Doctored images are stored in JPEG at the same quality '75'. Untouched 3600 JPEG images are also uncompressed and stored at the same quality '75'. Some untouched images and doctored at quality '75' are shown in Figure 2. Then both untouched and doctored images are transcoded to the quality of '40'. The task is set to discriminate the doctored images of quality '40' from the untouched of quality '40'.

We compare our detectors LF-DCT and LF-SEDCT to other detectors within the state-of-the-art, including cc-absNJ in the reference [10], the detectors designed in the references [18, 19, 20, 21], and the forgery detection method designed in [17] for detecting color image forgery, including the detectors Markov-Y/Cr/Cb and the combination Markov-YCrCb. Ensemble learning [8] that was designed for image steganalysis to deal with large scale features is applied to our proposed detectors.

Table I lists the mean accuracy over 30 experiments by applying the ensemble classifier in detecting untouched JPEG images (quality of '40') and doctored JPEG images (quality of '40'). In each experiment, 67% observations are randomly selected for training and other 33% observations are used for testing. The prediction outcomes of testing sets are classified as True Positive (TP), False Positive (FP), False Negative (FN), and True Negative (TN). The detection accuracy is given by 0.5*TP/(TP+FN)+0.5*TN/(TN+FP). Compared to the existing neighboring joint density feature set, cc-absNJ, the integration of spatial differential neighboring joint density and DCT domain-based marginal and neighboring joint density improve the detection accuracy by about 20%; compared to other methods, the detection accuracy is improved by about 40%.

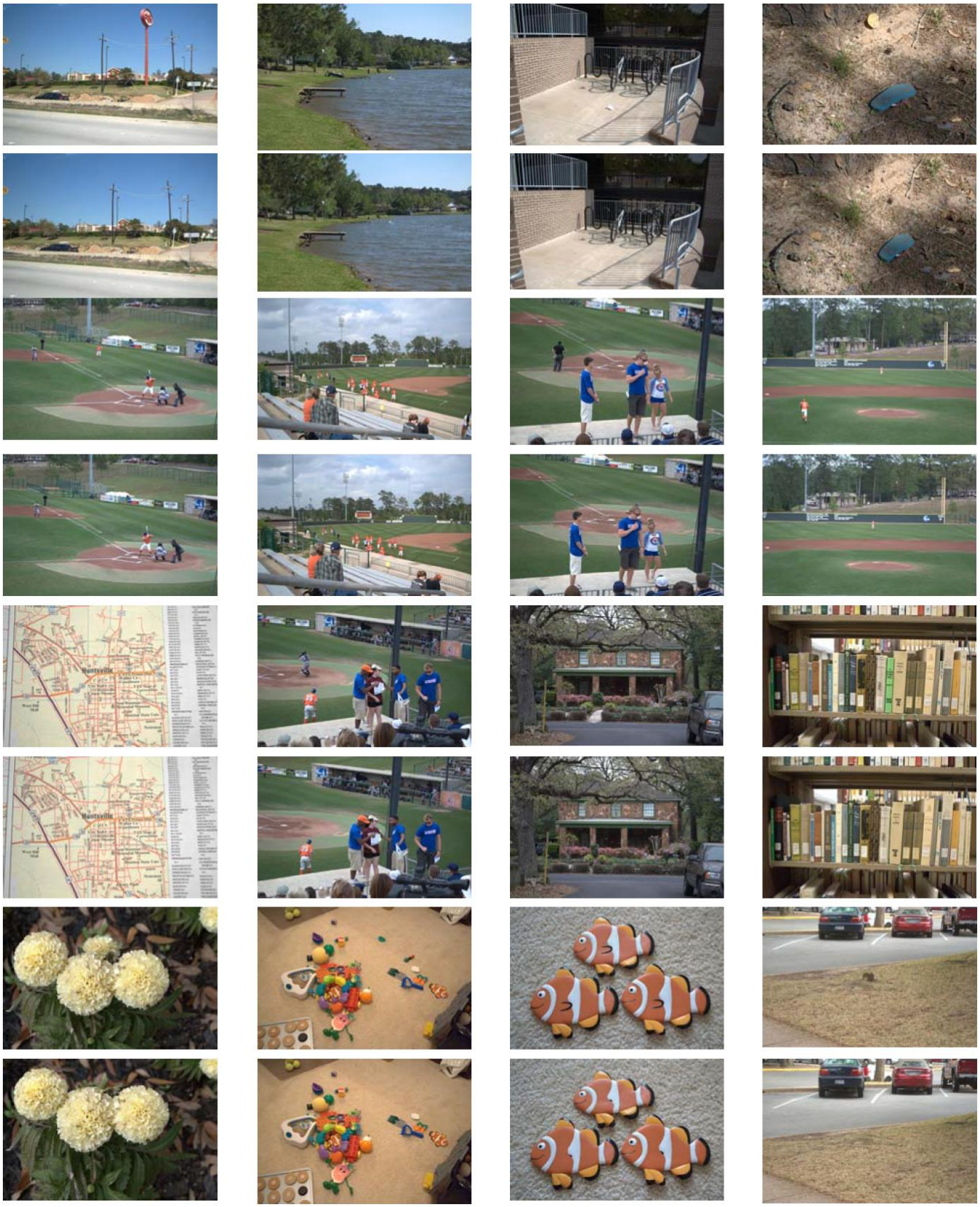

Figure 2. Examples of untouched images (odd rows) and doctored images (even rows) at the quality of '75'

TABLE I
DETECTION ACCURACY IN DISCRIMINATING SEAM CARVING FORGERY FROM UNTOUCHED IN LOW-LEVEL JPEG IMAGES (QUALITY OF 40)

Feature set or detection method	Detection accuracy (%)
Markov-Y [17]	51.1
Markov-Cr [17]	53.1
Markov-Cb [17]	53.1
Markov-YCrCb [17]	54.4
Chang et al. 2013 [18]	53.5
Yin et al. 2015 [21]	51.9
Wei et al. 2014 [20]	51.8
Ryu and Lee 2014 [19]	56.4
cc-absNJ [10]	74.5
LF-DCT	89.8
LF-DEDCT	94.1

Additionally, we test the classification accuracy in detecting the seam carving forgery under the recompression attack on the same quality of 75. Table II lists the mean detection accuracy. It also demonstrates the significant improvement in terms of the detection accuracy by proposed approach.

TABLE II
DETECTION ACCURACY IN DISCRIMINATING LOW-QUALITY SEAM CARVING FORGERY FROM UNTOUCHED IN JPEG IMAGES (QUALITY OF 75)

Feature set or detection method	Detection accuracy (%)
Markov-Y [17]	52.7
Markov-Cr [17]	56.3
Markov-Cb [17]	56.5
Markov-YCrCb [17]	62.2
Chang et al. 2013 [18]	63.9
Yin et al. 2015 [21]	55.4
Wei et al. 2014 [20]	51.9
Ryu and Lee 2014 [19]	64.4
cc-absNJ [10]	93.0
LF-DCT	94.4
LF-DEDCT	99.3

V. CONCLUSIONS

To expose the seam carving forgery under JPEG recompression attacks, which had not been well explored in literature, we design a hybrid large scale feature mining-based approach, consisting of over 100,000 features. Ensemble learning is adopted to deal with the high dimensionality and to recognize the patterns of untouched images and doctored from recompressed images at the same or lower quality. Our experiments demonstrate the effectiveness of proposed hybrid large feature mining-based approach.

The future may include more reasonable features including the distortion of the structural information that may be caused by seam carving. Feature selection and feature reduction will be carried out in our following study too.

ACKNOWLEDGMENT

The support for this study from NSF under the award CCF-1318688 is highly appreciated.

REFERENCES

[1] S. Avidan and A. Shamir (2007). Seam carving for content-aware image resizing. ACM Transactions on Graphics, 26(3), Article 10.

[2] T. Bianchi and A. Piva (2012). Detection of non-aligned double JPEG compression based on integer periodicity maps. IEEE Trans. Inf. Forensics Security 7(2): 842-848.

[3] Y. L. Chen and C. T. Hsu (2011). Detecting recompression of JPEG images via periodicity analysis of compression artifacts for tampering detection. IEEE Trans. Inf. Forensics Security, 6(2):396–406.

[4] H. Farid (2009). A survey of image forgery detection. IEEE Signal Processing Magazine, 26(2):16-25.

[5] H. Farid. (2009). Exposing digital forgeries from JPEG ghosts. IEEE Trans. Inf. Forensics Security, 4(1):154-160.

[6] C. Fillion and G. Sharma (2010). Detecting content adaptive scaling of images for forensics applications. In Proceedings of SPIE, Media Forensics and Security II, vol. 7541, doi: 10.1117/12.838647.

[7] J. Fridrich and J. Kodovsky J. (2012). Rich models for steganalysis of digital images. IEEE Transactions on Information Forensics and Security, 7(3): 868-882.

[8] J. Kodovsky, J. Fridrich and V. Holub (2012). Ensemble classifiers for steganalysis of digital media. IEEE Transactions on Information Forensics and Security, 7(2):432-444.

[9] Q. Liu, A. H. Sung and M. Qiao (2011). Neighboring joint density-based JPEG steganalysis. ACM Transactions on Intelligent Systems and Technology, 2(2): article 16.

[10] Q. Liu and Z. Chen (2014). Improved approaches with calibrated neighboring joint density to steganalysis and seam-carved forgery detection in JPEG images. ACM Trans. on Intelligent Systems and Technology, 5(4): article 63.

[11] W. Luo, Z. Qu, J. Huang and G. Qui (2007). A novel method for detecting cropped and recompressed image block. In Proc. of ICASSP 2007, vol. 2, pp. II–217–II–220.

[12] A. Sarkar, L. Nataraj and B.S. Manjunath (2009). Detection of seam carving and localization of seam insertions in digital images. In Proceedings of 11th ACM MM&Sec, pages 107-116

[13] Y. Q. Shi, C. Chen and W. Chen (2007). A Markov process based approach to effective attacking JPEG steganography. In Lecture Notes in Computer Science, vol.4437, pp. 249-264, 2007.

[14] http://en.wikipedia.org/wiki/Seam_carving.

[15] N. Dalal and B. Triggs (2005). Histograms of oriented gradients for human detection. In International Conference on Computer Vision & Pattern Recognition, vol. 2, 886–893.

[16] Q. Liu (2011). Detection of misaligned cropping and recompression with the same quantization matrix and relevant forgery. In Proc. 3rd International ACM workshop on Multimedia in Forensics and Intelligence, pages 25-30.

[17] W. Wang, J. Dong and T. Tan (2010), "Image tampering detection based on stationary distribution of Markov chain", Proc 17th International Conference on Image Processing, pages 2101-2104, September 2010.

[18] W. Chang, T.K, Shih, H. Hsu (2013), "Detection of seam carving in JPEG images", in: Awareness science and technology and ubi-media computing, international conference on IEEE, 2013, pp, 632-638.

[19] S. Ryu and H. Lee (2014), "Detecting trace of seam carving for forensics analysis", IEICE Trans. Inform. Syst. 2014, 97(5): 1304-1311.

[20] J. Wei, Y. Lin, Y. Wu (2014), "A patch analysis method to detect seam carved images", Pattern Recognition Letter, 36: 100-106, 2014.

[21] T. Yin, G. Yang, L. Li, D. Zhang and X. Sun (2015), "Detecting seam carving based image resizing using local binary patterns", Computers & Security, 55:130-141, 2015.